KIRTLANDIA®

The Cleveland Museum of Natural History

February 1994 *Number 48:3-21*

A Redescription of *Gymnotrachelus* (Placodermi: Arthrodira) from the Cleveland Shale (Famennian) of Northern Ohio, U.S.A.

Robert K. Carr
Museum of Paleontology
The University of Michigan
Ann Arbor, MI 48109-1079

Abstract

The relationships among selenosteid arthrodires are inadequately known. The recovery of new material for *Gymnotrachelus hydei* Dunkle and Bungart from the Cleveland Shale (Famennian) of northern Ohio, U.S.A., offers a unique insight into an important, but poorly known member of this group. Previous analyses of selenosteids have suggested that *Gymnotrachelus* represents either a basal member of the Selenosteidae or a taxon of unresolved affinities. The various studies have differed also in the taxa included within the family. The current redescription of *Gymnotrachelus* provides the foundation for a parsimony based cladistic analysis of Selenosteidae using multiple outgroups. In contrast to previous analyses, *Gymnotrachelus hydei* is a derived member of Selenosteidae, sister taxon to *Melanosteus* Lelièvre, Feist, Goujet, and Blieck. *Gymnotrachelus hydei* is characterized by: (1) distinct sensory line grooves bounded by a pronounced lip; (2) a rostral expansion of the preorbital plate over the rhinocapsular region; (3) a pineal plate overlapped by preorbital and central plates; (4) the presence of a gap between submarginal, suborbital, and postsuborbital plates and head shield; (5) anterior superognathals with two posterolateral longitudinal rows of denticles with each row possessing one to three denticles; (6) an inferognathal possessing a single row of denticles with one or two accessory rows posterolaterally; (7) an ovate leaf-shaped parasphenoid with a short stem-like prehypophysial region; (8) an anterior median ventral plate in the form of an isosceles triangle with equivalent length and width; (9) an anterior ventrolateral plate similar in shape to the posterior ventrolateral plate of *Heintzichthys gouldii* (a rounded scalene triangle with the base facing medially); and (10) overlap of the left posterior ventrolateral plate onto the right. *Brannosteus* Stensiö is considered here to be a member of Selenosteidae although further analysis is needed to confirm this relationship.

Introduction

The current description of *Gymnotrachelus hydei* is part of a continuing study of poorly known and undescribed specimens recovered from the Cleveland Shale (Famennian) of northern Ohio, U.S.A. *Gymnotrachelus hydei* was first described by Dunkle and Bungart (1939) based on a single incomplete specimen, preserved in part and counterpart, which had undergone some weathering with further loss of information. Dunkle and Bungart recognized a relationship between *Gymnotrachelus hydei* and selenosteid arthrodires; however, they did not provide a clear phylogenetic diagnosis. In 1965-1966, The Cleveland Museum of Natural History collected additional *Gymnotrachelus hydei* material during the Interstate 71 Paleontological Salvage Project. I here redescribe *Gymnotrachelus hydei* based on this new material, providing both an update of Dunkle and Bungart's description of *Gymnotrachelus hydei* and a new diagnosis. Finally, I review the phylogenetic relationships of *Gymnotrachelus* to other Selenosteidae, although the relationship of selenosteids to other aspinothoracid arthrodires remains unclear.

A number of workers have evaluated relationships among aspinothoracid arthrodires (Gross, 1932; Stensiö, 1963, 1969; Dunkle and Bungart, 1939; Obruchev, 1964; Denison, 1975, 1978; Lelièvre et al., 1987; Miles and Dennis, 1979; Gardiner, 1990; Gardiner and Miles, 1990; Carr, 1991). Early analyses often lacked phylogenetically informative diagnoses for taxa because of poor preservation and at the time a lack of separation between primitive and derived features. The primary sources for information on aspinothoracid arthrodires are based on materials from two localities: the upper Frasnian Kellwasserkalk of the *Manticoceras* Beds, Germany, and the upper Famennian Cleveland Shale, Ohio, U.S.A. During the Interstate 71 Paleontological Salvage Project (1965-1966) numerous specimens of new or poorly known taxa were recovered. Carr (1991; see also Denison, 1978; Lelièvre et al., 1987) noted insufficiencies in previous analyses of North American and European aspinothoracid arthrodires and provided a limited phylogenetic analysis based in part on undescribed material from The Cleveland Museum of Natural History. The current study of *Gymnotrachelus hydei* provides new data on a poorly known North American taxon that is important for more detailed analyses.

Anatomical abbreviations used in figures and listed at the end of the paper follow those of Dennis-Bryan (1987) and Carr (1991). Specimen number prefixes denote their respective institutions: CMNH, Cleveland Museum of Natural History, Cleveland, Ohio; PM, Peabody Museum, Yale University. The suffix "id" when used to form taxonomic adjectives does not refer to the familial level in Linnean classification, but is used as a convenience for discussing informal taxonomic units.

Methods

Phylogenetic hypotheses are based, in this discussion, on analyses using PAUP (v. 3.1, Swofford, 1993) and MacClade (v. 3, Maddison and Maddison, 1992). Parameters specified in PAUP include the exhaustive search option with all characters unordered and Trematosteidae and Brachydeiridae set as outgroups. The most parsimonious trees (minimal character transformations) are retained for the current discussion.

Systematic Paleontology

Placodermi McCoy, 1848
Arthrodira Woodward, 1891
Brachythoraci Gross, 1932
Eubrachythoracei Miles, 1971
Pachyosteina Denison, 1978
Aspinothoracidi Stensiö, 1959 (*sensu* Miles and Dennis, 1979)
Selenosteidae Dean, 1901
Gymnotrachelus Dunkle and Bungart, 1939

Diagnosis

Gymnotrachelus is a typical aspinothoracid arthrodire characterized by reduction of the lateral and occipital thickenings of the head shield and loss of the spinal plate. The genus is characterized by: (1) distinct sensory line grooves bounded by a pronounced lip; (2) rostral expansion of the preorbital plate over the rhinocapsular region; (3) a pineal plate overlapped by preorbital and central plates; (4) the presence of a gap between submarginal, suborbital, and postsuborbital plates and head shield; (5) anterior superognathals with two posterolateral longitudinal rows of denticles with each row possessing one to three denticles; (6) an inferognathal possessing a single row of denticles with one or two accessory rows posterolaterally; (7) an ovate leaf-shaped parasphenoid with a short stem-like prehypophysial region; (8) an anterior median ventral plate in the form of an isosceles triangle with equivalent length and width; (9) an anterior ventrolateral plate similar in shape to the posterior ventrolateral plate of *Heintzichthys gouldii* (a rounded scalene triangle with the base facing medially); and (10) overlap of the left posterior ventrolateral plate onto the right.

Type species

Gymnotrachelus hydei Dunkle and Bungart, 1939

Diagnosis

Same as genus.

Holotype

CMNH 5724. Figure 1 depicts a redrawing of Dunkle and Bungart's (1939) camera lucida drawing of the holotype corrected to reflect current plate interpretations.

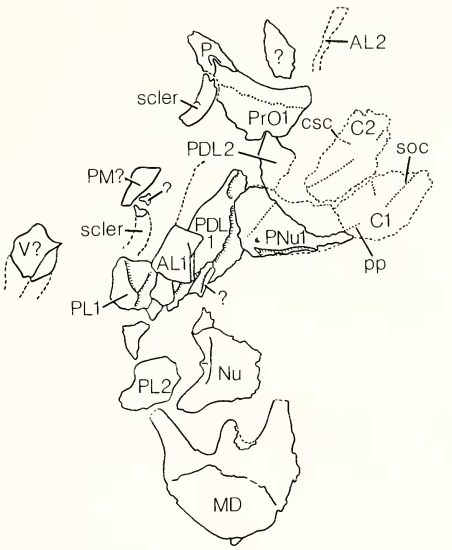

Figure 1. *Gymnotrachelus hydei.* A reinterpretation of Dunkle and Bungart's (1939, fig.1) camera lucida drawing of the holotype CMNH 5724. Structures and archaic terminology are updated based on the current analysis. A numerical postscript of 1 = left and 2 = right.

Additional Material

PM 55665, articulated anterior part of head shield in internal view, isolated suborbital, and inferognathal impression (Figure 3); CMNH 8049, disarticulated thoracic shield, in part, with scapulocoracoid, cheek with sclerotics, and gnathals; CMNH 8050, nearly complete head and thoracic shields in internal view with cheek (including sclerotics) and gnathal plates (Figures 8E, 12B & C); CMNH 8051, disarticulated posterior head shield, cheek with sclerotics, incomplete thoracic shield, and inferognathal (Figures 4B & C, 5, 6, 7B, 8A & B, 11); CMNH 8052, incomplete disarticulated head and thoracic shields, sclerotics, parasphenoid (Figures 4A, 4D & E, 9B, 10); CMNH 8053, gnathals, isolated fragments of head and thoracic shields and cheek (Figures 4F, 9A); CMNH 8054, incomplete, but partially articulated head shield, disarticulated and incomplete cheek with sclerotics and thoracic shield, and inferognathals (Figure 12A & D); CMNH 8055, incomplete cheek with sclerotics, gnathals, one plate and fragment from thoracic shield (Figures 7A, 8D); CMNH 8084, incomplete right inferognathal (posterior occlusal region and blade); CMNH 8776, incomplete left inferognathal (Figure 8C); CMNH 8778, 8779, and 8788, isolated left posterior superognathals; CMNH 8798, incomplete left suborbital plate; and CMNH 8799, incomplete disarticulated head and thoracic shields, cheek with sclerotics, and fragmented scapulocoracoids.

Occurrence

All material was found within the Cleveland Shale Member (Famennian) of the Ohio Shale, northern Ohio, U.S.A. The holotype was found on Townes Creek, Lorain County, Ohio. Interstate 71 material was recovered from the *Heintzichthys* zone (Carr, 1991) which was quarried at the intersection of West 130th Street and Interstate 71, Cleveland, Ohio. PM 55665 is recorded only as being found in the Cleveland Shale.

Description

Head Shield

General features. The head shield is composed of 15 plates (Figure 2A & B). Of these, six are paired with three unpaired median plates. There is no evidence for the presence of postnasal or internasal plates. Grooves for sensory lines are present and follow the typical arthrodiran pattern; however, they are bounded by a well-developed lip or ridge. Although ridge prominence is variable within an individual, this character is found consistently within all specimens. This condition is distinctive for *Gymnotrachelus* among aspinothoracid arthrodires within the Cleveland Shale fauna and is apparently not a simple consequence of bone compression during preservation. All plates are flattened, making interpretations of original curvature difficult.

Rostral (R). A definitive rostral plate is not recognized in any of the specimens. On the basis of the size and shape for the gap between preorbital plates, the rostral plate if present appears to have been triangular in shape with a broad anterior margin (Figures 2A, 3). The presence of a rostral plate is speculative since there is no evidence for either the plate or overlap areas on adjacent plates.

Pineal (P). The pineal plate (Figure 2A) is exposed ventrally in the type (CMNH 5724, Figure 1) and PM 55665 (Figure 3) and exposed externally in CMNH 8052 (Figure 4A) as an isolated plate. The latter specimen has bilateral overlap areas for the central plates (oa.C, Figure 4A) and reduced overlap areas for the preorbital plates (oa.PrO, Figure 4A). In contrast, in *Heintzichthys gouldii* the pineal overlaps both preorbital and central plates while in *Dunkleosteus terrelli* the pineal overlaps central and rostral plates, but is overlain by the preorbital. A central anterior extension of the pineal plate suggests that this plate may have contacted the rostral. This central extension is much narrower than that suggested by Dunkle and Bungart (1939, p. 17). No external overlap

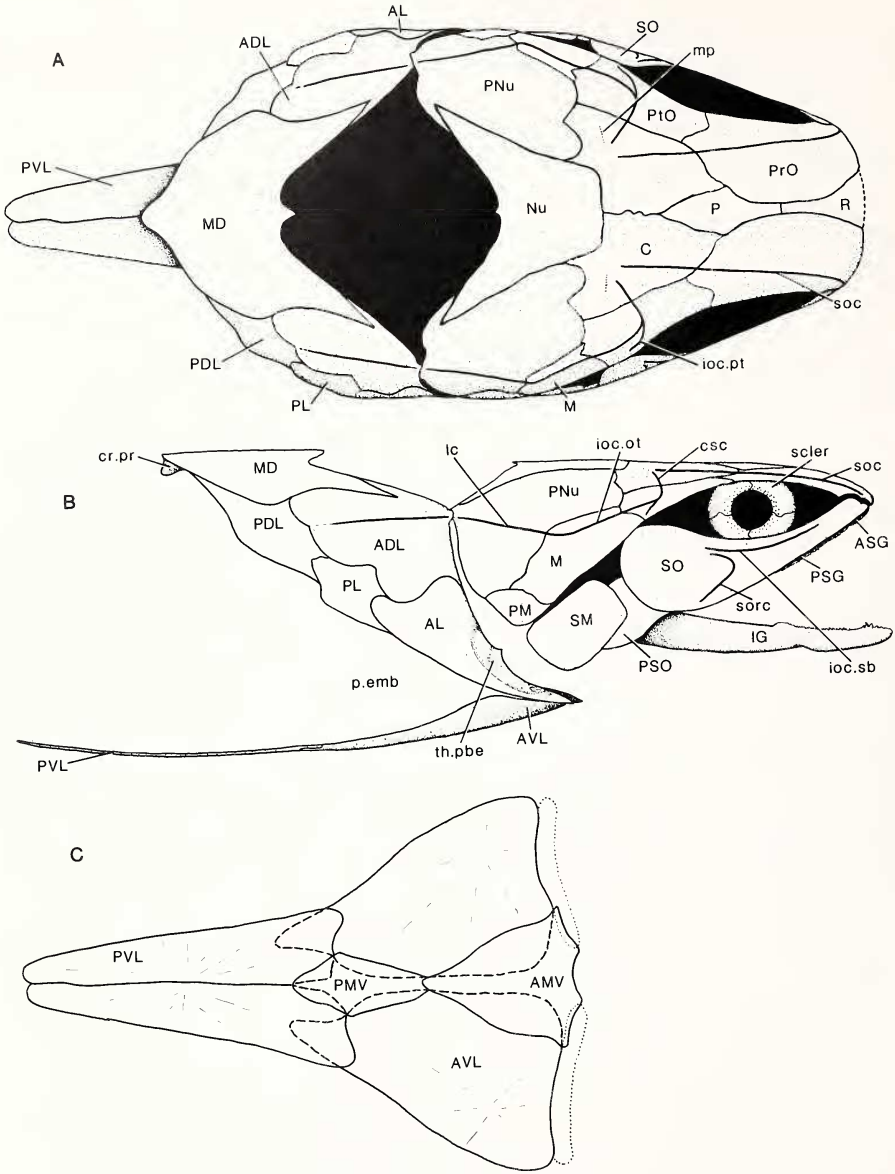
A
AL
ADL
SO
mp
PNu
PtO
PVL
PrO
MD
Nu
P
R
C
soc
PDL
ioc.pt
PL
M
B
cr.pr
MD
lc
ioc.ot
csc
scler
soc
PNu
PDL
ADL
M
SO
ASG
PSG
PL
PM
SM
sorc
AL
IG
PSO
ioc.sb
p.emb
th.pbe
AVL
PVL
C
PVL
PMV
AMV
AVL

area for the rostral plate is discernible and internally exposed pineal plates do not reveal the anterior region, preventing evaluation for the presence of a rostral contact face. Internally the pineal fossa is bounded posteriorly by a well-developed ridge. A pineal foramen is present externally (Figure 4A).

Nuchal (Nu). The nuchal (Figures 2A & B; 4B & C) is embayed posteriorly with a small process in the midline (p.pr, Figure 4C). In CMNH 8050, the median process is elongate, extending *ca.* 8 mm beyond the posterior margin of the head shield. Long slender alae extend posterolaterally along the nuchal gap. The anterior border of the nuchal is transverse.

The internal nuchal thickening (n.th, Figure 4B) is reduced and limited to the central region. The thickening continues as thin ridges forming the descending faces of the posterolateral alae. Paired pits (pt.u, Figure 4B) open posteriorly and are separated by a median septum (m.sept, Figure 4C) which is continuous with the posterior median process. Distinct muscle pits are absent (f.lv, Goujet, 1984) with muscle insertion limited to two laterally extended shelves or elongate fossae (f_e.lv, Figure 4C).

Preorbital (PrO). The preorbital plate (Figures 2A & B; 3) possesses a preorbital process, although it is not pronounced laterally due to the large orbit and gentle curvature of the dorsal orbit border (contrast this with *Dunkleostens* where distinct pre- and postorbital processes denote a smaller orbit with a pronounced curvature). A groove for the supraorbital sensory line traverses the plate and ends near the anterolateral corner (soc, Figures 2A & B). The ratio of longitudinal lengths of the preorbital and central plates is *ca.* 1.1 (PrO/C); the ratio of lengths of the preorbital and postorbital plates is *ca.* 1.2 (PrO/PtO).

Internally, a supraorbital vault (suo.v, Figure 3) is present extending from the preorbital process onto the postorbital plate. Medially, the supraorbital vault shows a recess for the neurocranial preorbital process (ch.pro.pr, Figure 3). Anterior to this recess, a supraethmoid crista is present, but forms a low platform versus a distinct ridge.

Figure 2. *Gymnotrachelus hydei.* Composite reconstructions of head and thoracic shields in A, dorsal view and B, lateral view. Only a few head shield plates are complete in all dimensions; therefore, plate boundaries are reconstructed based on known plate components and potential boundaries and plate overlaps with adjacent plates. The posterior margin of the central and anterior dorsolateral plates are incompletely known. C, a reconstruction of the ventral thoracic plates in dorsal view (no attempt has been made to interpret original curvature). Estimated boundaries for the interolateral plates are drawn in dotted lines. Hidden plate boundaries are drawn in dashed lines.

Figure 3. *Gymnotrachelus hydei.* Internal view of an incomplete head shield (PM 55665). Scale bar equals 1 cm.

This platform is confined to the preorbital plate and does not extend medially as does the crista in some European selenosteids (e.g., *Enseostens,* Stensiö, 1963, fig. 113A). The preorbital plate is expanded anteriorly over the rhinocapsular region (Figure 3; also seen in *Heintzichthys gouldii,* but to a lesser degree, Carr, 1991, fig. 3A; a similar region is seen in tubular snouted coccosteomorphs *Rolfosteus* and *Tubonasns,* Dennis and Miles, 1979). Due to flattening in preservation, it is not clear whether this expansion is downturned in life. Along the plate's lateral margin, there is a shallow notch between the preorbital dermal process and the anterolateral extension over the rhinocapsular region. The supraorbital sensory line groove is detected internally as a raised ridge on the preorbital plate (Figure 3).

Postorbital (PtO). The postorbital plate (Figures 2A & B, 3, 4D) lacks a postorbital process. Grooves for three sensory lines are present on the postorbital plate; central sensory line (csc, Figure 4D) and postorbital and otic branches of the infraorbital sensory line (ioc.pt and ioc.ot respectively, Figure 4D). The central sensory line and the otic branch of the infraorbital line are generally continuous, forming an angle of *ca.* 95°, although they are disjunct on the right postorbital plate in CMNH 8052 (conjoined on the left). The postorbital branch of the infraorbital line does not always unite with the former two sen-

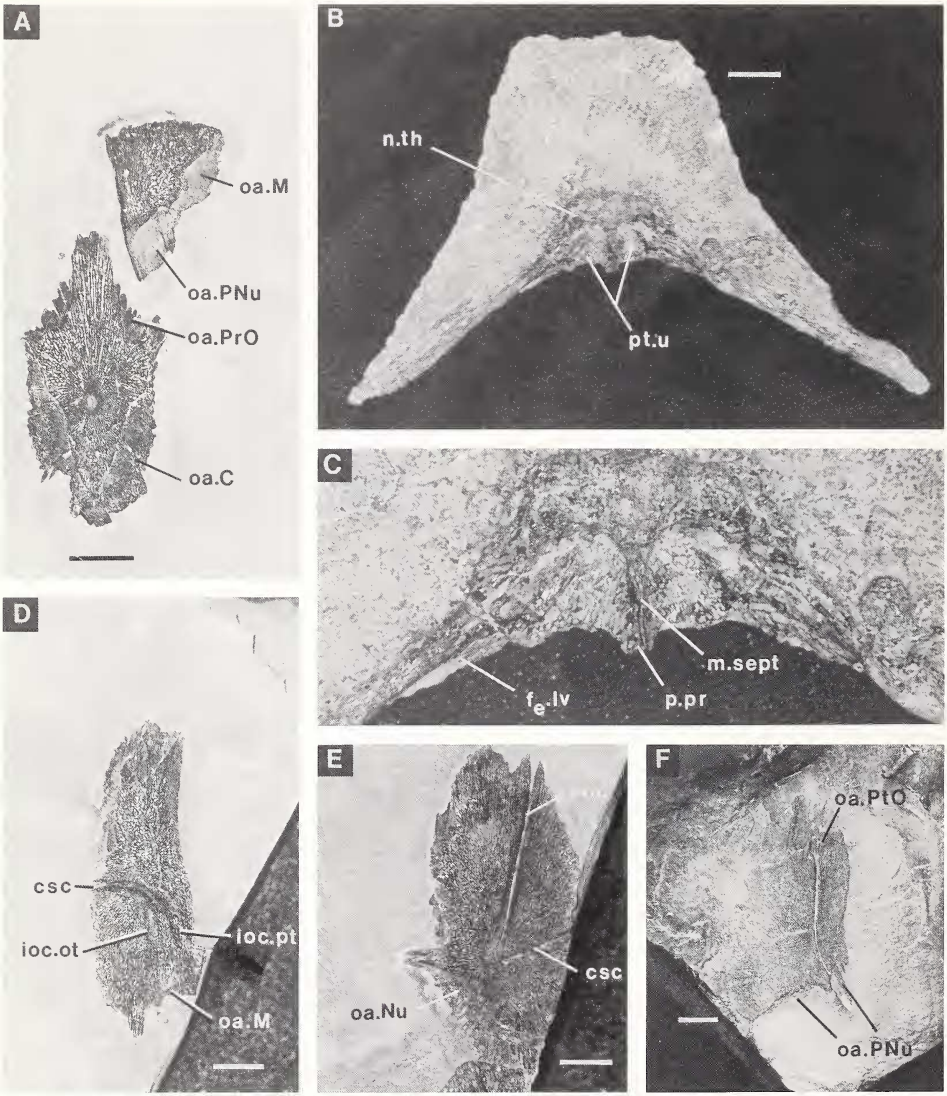

Figure 4. *Gymnotrachelus hydei.* A, pineal (lower left) and left postmarginal plates (CMNH 8052) in external view. B, nuchal plate in internal view and C, close-up of nuchal thickening (CMNH 8051). D, right postorbital plate in external view (CMNH 8052). E, right central plate in external view (CMNH 8052). F, left marginal plate in external view (CMNH 8053). Scale bars equal 1 cm.

sory lines and is directed posteriorly. The angle formed between the otic and postorbital branches is *ca.* 30-40°. Dunkle and Bungart (1939) noted a short postorbital branch of the infraorbital sensory line groove. They suggested that it continued onto the marginal plate based on the presence of a marginal plate overlap area at the termination of the postorbital branch groove (Dunkle and Bungart, 1939, om.m, fig. 2). The interpretation of a marginal plate overlap area and a postorbital process appear to be in error. The putative postorbital process is located well anterior to the supraorbital crista. The overlap area appears to be a depression on the postorbital plate associated with a continuation of the postorbital branch of the infraorbital sensory line. A distinct overlap area for the marginal plate is seen in CMNH 8052 (oa.M, Figure 4D).

The central-postorbital plate length ratio is *ca.* 1.2 (C/PtO). Internally, the supraorbital vault is continued posteriorly. A distinct, low ridge forms the medial boundary of the vault and continues posterolaterally as a supraorbital crista to the lateral margin of the plate. There is no apparent inframarginal crista extending posteriorly from the supraorbital crista on the postorbital plate.

Central (C). The central plates (Figures 2A & B, 3, 4E) are elongate with the posterior margin incompletely preserved in available material. They are separated anteriorly by the pineal plate, are joined along a sinuous suture for *ca.* 33% of their longitudinal length, and are separated posteriorly by the nuchal plate. Two distinct sensory lines are present; a supraorbital sensory line (soc, Figure 4E) and a central sensory line (csc, Figure 4E). A middle pit-line may be occasionally present and is noted only on CMNH 8054 (seen on the right central plate impression and externally on the left central plate). It is directed posterolaterally from the ossification center forming an angle of *ca.* 35° with the central sensory line. This line appears to be distinct from the "middle head line" of Dunkle and Bungart (1939, i.ac.sc, fig. 1) which, if correctly identified as a sensory line, is more likely a posterior pit-line. A posterior pit-line is not seen on any of the new material and a middle pit-line, as noted above, is found only on CMNH 8054.

A low endolymphatic thickening is present internally at the ossification center and unlike *Dunkleosteus* and *Heintzichthys* is not continuous with the nuchal thickening. The raised ridge indicating the course of the supraorbital sensory line groove on the preorbital plate's internal surface is continued onto the central plate (Figure 3). There is no distinct boundary for the insertion of the cuccularis muscle (compare with the depression for the cuccularis muscle in *Dunkleosteus*, dp.m.cu, Stensiö, 1963, fig. 112A).

Marginal (M). The marginal plate (Figures 2A & B, 4F) possesses a single sensory groove; a continuation of the postorbital branch of the infraorbital line, which becomes the main lateral line on the paranuchal plate. The boundary between these lines is typically demarcated by the presence of a postmarginal line extending from the ossification center; however, there is no evidence for the presence of a groove for this line in *Gymnotrachelus*. Dunkle and Bungart (1939, p.18, fig. 6A & C) interpreted a single plate fragment with a sensory line as the marginal plate in the holotype (CMNH 5724). This piece is interpreted here as a fragment of the right preorbital

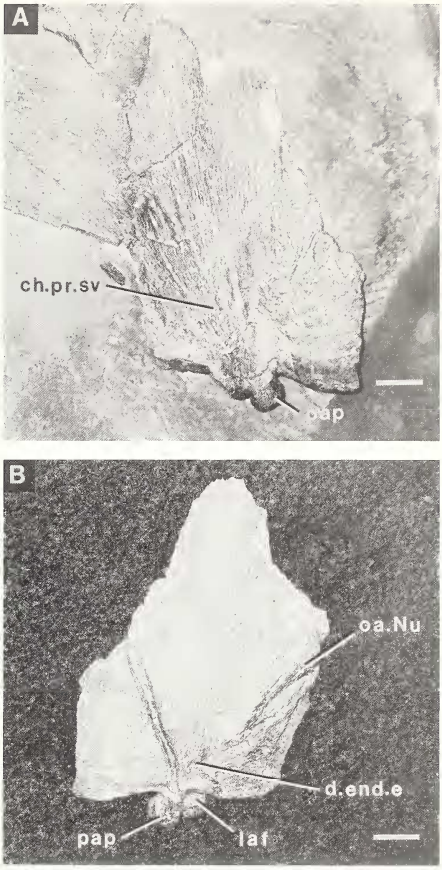

Figure 5. *Gymnotrachelus hydei*. Left paranuchal plate in A, internal and B, external views (CMNH 8051). Scale bars equal 1 cm.

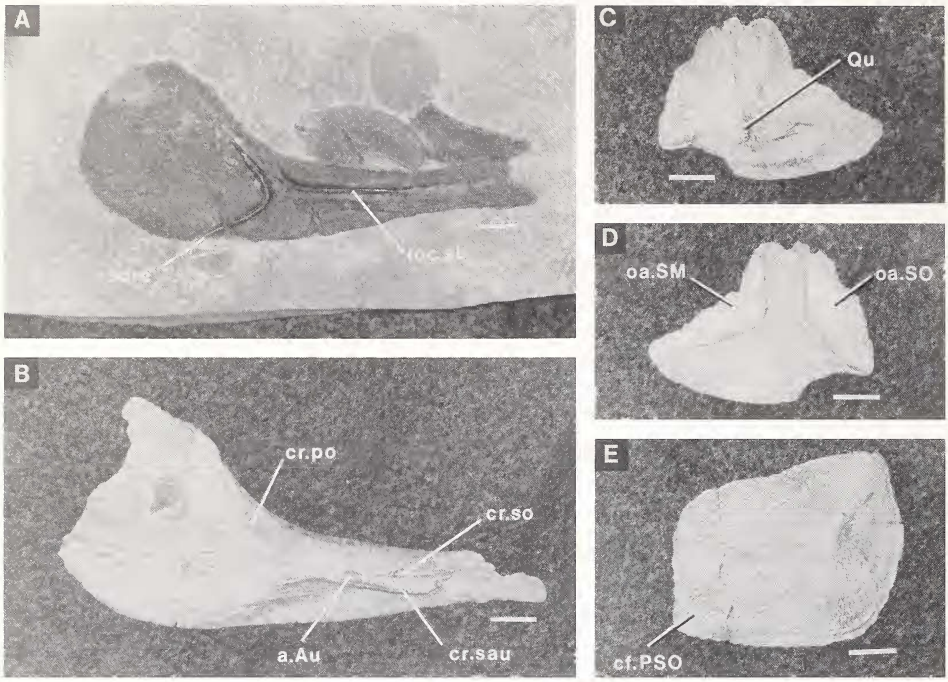

Figure 6. *Gymnotrachelus hydei* (CMNH 8051). Suborbital plate in A, right external and B, left internal views. Right postsuborbital plate in C, internal and D, external views. E, right submarginal plate in internal view. Scale bars equal 1 cm.

plate possessing thickenings associated with the dermal preorbital process. On the marginal plate, the sensory line groove is situated near and parallel to the plate's medial border.

It is difficult to evaluate the presence of a central and marginal plate contact; however, the general spacing of plates suggests a lack of contact. Two overlap areas are present on the marginal plate, an anterior postorbital plate (oa.PtO, Figure 4F) and a posterior paranuchal plate overlap (oa.PNu, Figure 4F). Internally, a low inframarginal crista parallels the external sensory line to the plate's ossification center. At this point, a thickening continues beneath the main lateral line, while the inframarginal crista continues as a low thickening (barely noticeable in CMNH 8051) to the posteroventral corner of the plate and onto the postmarginal plate.

Postmarginal (PM). Two isolated postmarginal plates are preserved, one in CMNH 8052 and the other in CMNH 8799. The postmarginal plate (Figures 2B, 4A) is triangular in shape with anteroventral and posteroventral borders forming a *ca.* 90° angle. A distinctive subobstantic region is absent; however, a thinning of the posteroventral margin is noted in CMNH 8799. The contact margins of neighboring plates are not present in the two specimens with postmarginals preserved, hindering the interpretation of overlap areas. However, the marginal plate shape and orientation of an internal inframarginal crista suggest the presence of overlap areas for the paranuchal (oa.PNu, Figure 4A) and marginal (oa.M, Figure 4A) plates with the latter being larger. Internally, a continuation of the inframarginal crista is present.

Paranuchal (PNu). The paranuchal plate (Figures 2A & B; 5) possesses a postnuchal process that extends onto the descending posterior face of the head shield. An overlap area for the nuchal plate is present (oa.Nu, Figure 5B) which is partially overlain by the postnuchal process forming a recess for the nuchal plate's posterolateral ala. The main lateral line traverses the plate ending along the posterior margin just above the junction of

Figure 7. *Gymnotrachelus hydei*. A, sclerotic plate in external view (CMNH 8055). Scale bar equals 1 cm. B, close-up of external ornamentation (CMNH 8051). Scale bar equals 0.5 cm.

the lateral articular fossa (laf, Figure 5B) and occipital para-articular process (pap, Figures 5A & B). An external opening for the endolymphatic duct is present (d.end.e, Figure 5B). The lateral articular fossa is well developed with the occipital para-articular process being short and nearly round.

Internally, there is a distinct channel (ch.pr.sv, Figure 5A) and recess for the dorsal aspect of the supravagal process of the neurocranium. The channel extends posteriorly to the ventral lip of the lateral articular fossa and is directed toward the base of the occipital para-articular process.

Cheek Plates

General features. The three plates (suborbital, postsuborbital, submarginal) of the cheek are not fused to the head shield. As in the head shield, sensory line grooves are bounded by a well-developed lip (ridge). All plates have been flattened secondarily.

Suborbital (SO). The shape of the suborbital plate (Figures 2B, 6A & B) is similar to that of other selenosteids, with the posterior region narrowing gently to form an anterior "handle." The posterior "blade" region is round. The ventral border of the orbit forms a shallow concavity. The groove for the supraoral sensory line (sorc, Figure 6A) forms a closed angle (*ca.* 85°) and does not join with the groove for the suborbital branch of the infraorbital line (ioc.sb, Figure 6A). The suborbital branch groove ends before the anterior extension of the "handle" (a distance of approximately one quarter of the total length of the suborbital plate). The groove parallels the internal suborbital crista (cr.so, Figure 6B) and separates the "handle" into two asymmetrical regions, the ventral region being larger (in *Dunkleosteus* and *Heintzichthys* the position of the groove is closer to the ventral margin).

Internally there is a subocular shelf (cr.so, Figure 6B) and subautopalatine (cr.sau, Figure 6B) and postorbital (cr.po, Figure 6B) cristae. There is no contact face for a posterior superognathal on the subautopalatine crista. This ventral ridge extends posteroventrally as a low ridge onto the "blade" portion of the suborbital plate (= R3 of Heintz, 1932, fig. 22). The subocular and postorbital cristae are continuous.

Postsuborbital (PSO). The postsuborbital plate (Figures 2B, 6C & D) is triangular with distinct overlap areas for the suborbital (oa.SO, Figure 6D) and submarginal (oa.SM, Figure 6D) plates. The shape of the suborbital overlap reflects the rounded posterior dimensions of the suborbital plate, whereas the submarginal overlap area forms an open angle (*ca.* 100°). These overlaps are separated dorsally resulting in a gap between the suborbital and submarginal plates and the head shield (Figure 2B). An anteroventral notch is present along the postsuborbital plate margin in CMNH 8054 (Figure 6C & D); however, in other specimens, the ventral margin forms a gentle sigmoid curve without a distinctive notch.

On the internal surface, a small thickening denotes the position of the quadrate (Qu, Figure 6C). Above the thickening, two low ridges suggest the trajectory of the palatoquadrate. The quadrate and ridges lie beneath the central region between external overlap areas suggesting that the palatoquadrate traverses beneath the gap between suborbital, postsuborbital, and submarginal plates and head shield.

Submarginal (SM). The submarginal plate (Figures 2B, 6E) is rectangular to subrectangular (in contrast to the elongate submarginal plate of primitive aspinothoracid arthrodires) and loosely abuts an overlap area on the postsuborbital. The ossification center is located posterodorsally (a posterior location is typical of eubrachythoracid

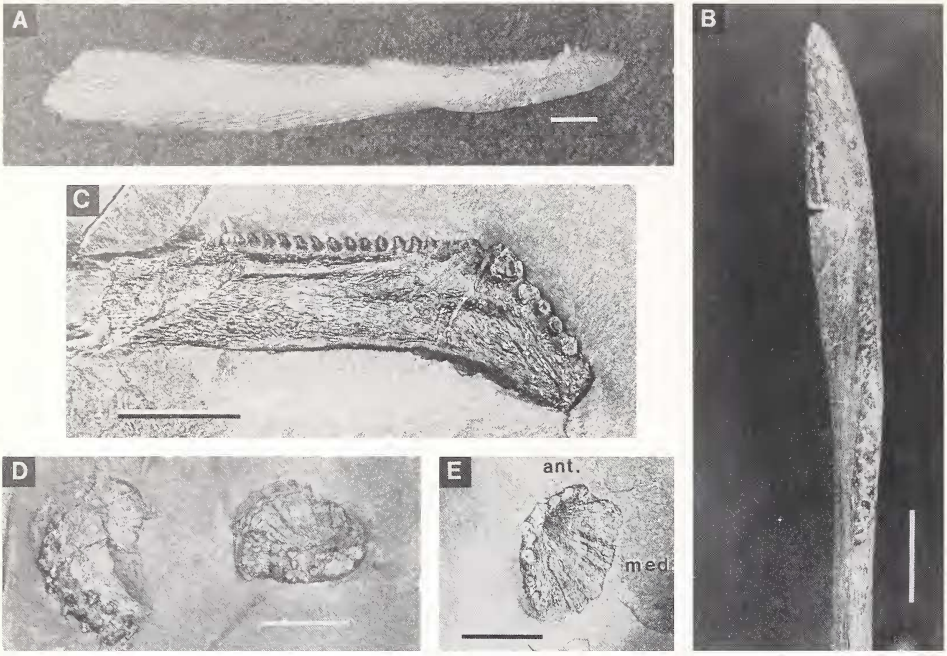

Figure 8. *Gymnotrachelus hydei.* Right inferognathal in A, lateral view and B, close-up of occlusal surface in dorsal view (CMNH 8051). C, close-up of left inferognathal in medial view (CMNH 8776). D, right and left anterior superognathals in ventral view (CMNH 8055). Note paired lateral rows of denticles. E, right anterior superognathal in ventral view (CMNH 8050). Scale bars equal 1 cm.

submarginal plates). Internally, the posterior margin shows growth ridges. A shallow contact face (cf.PSO, Figure 6E) is present at the anteroventral corner. A low ridge is present from the posterodorsal corner through the center of ossification and a short distance beyond. There is no groove for the hyomandibula.

Sclerotic (scler). There are four sclerotic plates (Figures 2B, 7) per eye. Typically, each sclerotic has an external overlap area and an internal contact face at opposite ends for adjacent sclerotic plates, although the nature of contact is variable (e.g., overlap areas at each end or both a contact face and overlap area at one end). Each sclerotic possesses an ornament of punctate denticles (Figure 7). These are densest medially and extend across the surface of the sclerotic. The lateral extent of denticles is variable both within and between specimens ranging from denticles only on the median edge to complete coverage.

Gnathal Plates and Parasphenoid

General features. Three paired gnathal elements are present (inferognathal, anterior and posterior superognathals). The anterior superognathals do not articulate with the parasphenoid, which is poorly preserved. All plates have been flattened secondarily.

Inferognathal (IG) (Figures 2B, 8A-C). The occlusal and adsymphysial region occupy *ca.* 46% of the total inferognathal length (44-48%). Anteriorly, the adsymphysial region possesses 5-6 large denticles in a single row. Typically the largest denticle is found at the posterior apex of the adsymphysis. Posterior to this cusp, the occlusal surface possesses a single row of evenly spaced denticles extending to the posterior margin of the occlusal region. The anterior denticles are recurved where not worn. In the posterior 40% of the occlusal region, one or two additional lateral rows of denticles are present (Figure 8B & C). The denticles within an individual inferognathal are spaced equally along the occlusal surface (5-10 denticles per centimeter). The number of denticles per centimeter varies inversely with overall size, and therefore

varies with age of the individual.

Anterior superognathal (ASG). The anterior superognathal (Figures 8D & E, 9A) is oval with 7-9 denticles arranged along the anterior and lateral margins. The anterior 3-4 denticles form an angle with the posterolateral denticles of *ca.* 120-130°. Anterior denticles typically form a single row with occasional accessory denticles. The lateral row is often bifid with denticles in each fork occasionally possessing up to two accessory denticles (Figure 8D; CMNH 8050 has only a single lateral row, Figure 8E). The bulk of the plate is represented by a medial lamina. A posterior process is absent.

Posterior superognathal (PSG). The posterior superognathals (Figure 9A) are elongate and crescent shaped. They are triangular in cross-section with the apex located dorsolaterally. A single row of denticles is located on the lateral convex margin of the flattened ventral surface (Figure 9A). Denticle number is variable and often difficult to discern due to worn or missing denticles (19-29 denticles; 3-5 denticles per centimeter anteriorly and 5-8 posteriorly: the 18 denticles reported by Dunkle and Bungart, 1939, represent an incomplete plate). At *ca.* 40% of the total length from the anterior margin, there is a shallow "step" extending from the ossification center anteromedially (Figure 9A). This "step" separates the lower and wider anterior region from the posterior region (the "step" may be homologous to the posterior process of the posterior superognathal plate in other arthrodires).

No single specimen possesses a complete inferognathal and set of superognathals. Anterior and posterior superognathals from CMNH 8055 and 8053 equal or exceed combined dimensions for adsymphysial and occlusal regions in any single inferognathal. This suggests that the anterior and lateral denticles of the anterior superognathal occlude with the adsymphysial region of the inferognathal. The most posterior denticles probably extend just beyond the apical denticle of the inferognathal (this is comparable to the condition in *Dunkleosteus* where the anterior superognathal occludes anteromedially and posterior to the anterior cusp of the inferognathal). The inferognathal adsymphysial denticles probably fit between the two posterior rows of denticles on the anterior superognathal. Denticles of the posterior superognathal occlude with the main inferognathal occlusal surface.

Parasphenoid. An incomplete and poorly preserved plate is interpreted as a parasphenoid in CMNH 8052 (Figure 9B). The parasphenoid is ovate leaf-like in shape with a short "stem" and a long narrow "leaf" (overall length/width = *ca.* 2.6). On the basis of comparisons with *Melanosteus* (Lelièvre et al., 1987), the "stem" is interpreted as the prehypophysial region (pre.reg, Figure 9B). The specimen is preserved in dorsal view with most of the plate missing revealing an impression of the ventral surface. Several punctate depressions suggest the presence of denticles.

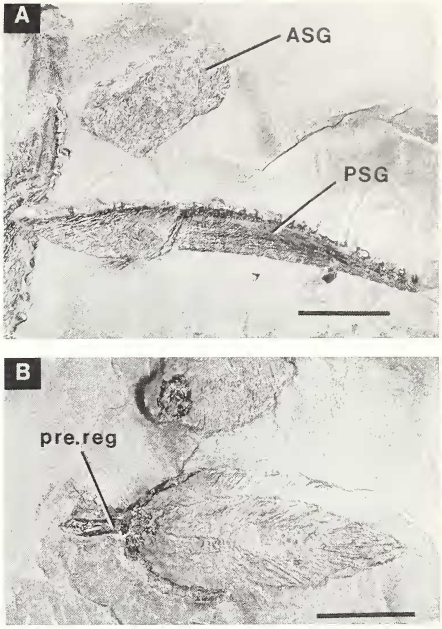

Figure 9. *Gymnotrachelus hydei.* A, left posterior superognathal in ventral view and an anterior superognathal in dorsal view (CMNH 8053). B, incomplete parasphenoid in dorsal view showing an impression of the ventral surface (CMNH 8052). Scale bars equal 1 cm.

Dermal Shoulder Girdle

General features. The dermal shoulder girdle is composed of 17 individual plates; three unpaired median plates (median dorsal, anterior and posterior median ventrals) and seven paired plates (anterior dorsolateral, posterior dorsolateral, anterior lateral, posterior lateral, interolateral, anterior and posterior ventrolaterals). The spinal plate is assumed to have been lost phylogenetically. A poorly preserved interolateral is recognized in a single specimen. Lateral line grooves possess a well-developed lip. All plates have been flattened secondarily.

Median dorsal (MD). The median dorsal plate (Figures 2A & B, 10) is rounded posteriorly with a small median process. The anterior margin forms a rounded W-shape with a central process ranging from *ca.* 16.7% (CMNH 8049) to *ca.* 60% (CMNH 8051) the length of the lateral alae. A lateral embayment is formed at the junction of the anterior ala and posterior rounded region. These embay-

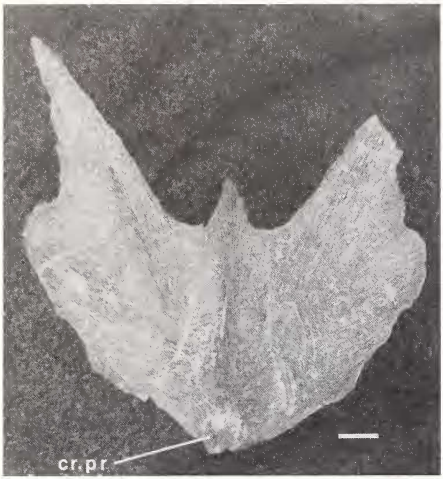

Figure 10. *Gymnotrachelus hydei* (CMNH 8052). Median dorsal plate in ventral view. Scale bar equals 1 cm.

ments are reminiscent of the condition seen in *Titanichthys* and *Bungartius* (Denison, 1978, fig. 80 and fig. 81 respectively). The projecting anterolateral corners of the posterior region overlap the posterior dorsolateral plates.

A carinal process (cr.pr, Figure 10) projects beyond the posterior border of the median dorsal plate. Internally, the carinal process begins as a low thickening on the central anterior process. The carinal process lacks a posterior concavity (spatulate forms include, e.g., *Dunkleosteus* and *Heintzichthys*). Beginning at the posterior third, the keel possesses a ventral groove that extends onto the posterior process. The median dorsal plate is further strengthened internally by paired thickenings radiating from the posterior base of the carinal process to the paired alae and along the posterolateral margins to the anterior areas of overlap for the posterior dorsolateral plates (to the rounded processes just posterior to the lateral notches). Contact faces are not discernible.

Anterior dorsolateral (ADL). The anterior dorsolateral plate (Figures 2A & B; 11D) carries the continuation of the main lateral line groove. Two overlap areas are present: a narrow anterodorsal area for the ala of the median dorsal plate (oa.MD, Figure 11D) and an anteroventral area for the anterior lateral plate (oa.AL, Figure 11D). The overall shape is difficult to infer since the thin posterior margin is incomplete. Piecing together a shape based on overlap areas on adjacent plates (CMNH 8051) suggests that the posterior margin is three-pronged (dorsal, middle, and ventral extensions). First, there is a dorsal extension possessing the median dorsal overlap and contacting the posterior dorsolateral plate. Second, a middle extension lies within the anterior dorsolateral overlap area on the posterior lateral plate (this overlap is variable in some specimens suggesting less of a distinction between the dorsal and middle extensions on the posterior margin of the anterior dorsolateral plate). Finally, there is a ventral extension possessing an overlap area for the anterior lateral plate. On the anterior margin, there is a well-developed condyle (kd, Figure 11D). Internally, a subglenoid process is present.

Posterior dorsolateral (PDL). The posterior dorsolateral plate (Figures 2A & B, 11C) is triangular (height/base = *ca.* 2.4 measured along the greatest dimension and its perpendicular dimension at the base). The posterior margin possesses a shallow process. Two distinct overlap areas are present on the external surface, an anterodorsal area for the median dorsal plate (oa.MD, Figure 11C) and an anteroventral one for the anterior dorsolateral plate (oa.ADL, Figure 11C). Both the posterior dorsolateral and posterior lateral plates in CMNH 8051 (Figure 11C & E) possess depressed regions on their external surfaces associated with their junction. Although there appears to be an overlap area on the posterior dorsolateral plate for the posterior lateral plate, this depression most likely represents a secondarily collapsed recess for the insertion of the posterior lateral plate (rec.PL, Figure 11C).

Anterior lateral (AL). The anterior lateral plate (Figures 2B, 11A & B) is widest dorsally and tapers to the anteroventral angle (av.w, Figure 11A). There is no evidence for the presence of a spinal plate. A medial lamina is present below a variably thickened postbranchial embayment (th.pbe, Figure 11A; erroneously labeled "prebranchial thickening" in Carr, 1991). A small pointed process extends anteriorly from the postbranchial thickening (Figure 11B, broken off, but reconstructed based on other specimens). Internally, the anterodorsal margin is thickened where the plate contacts the overlap area on the anterior dorsolateral plate. A small recess (rec, Figure 11B, partially obscured by a pyrite nodule, pyr., Figure 11B) is formed between the anterodorsally thickened margin and the pointed process on the postbranchial thickening. This recess probably housed the posteroventral corner of the head shield.

Posterior lateral (PL). The posterior lateral plate (Figures 2B, 11E) is taller than wide (height/width = *ca.* 1.7 along greatest dimension). The posterior margin possesses a rounded process. Anteroventrally, there are overlap areas for the anterolateral (oa.AL, Figure 11E) and anterior dorsolateral (oa.ADL, Figure 11E) plates (on the type specimen the anterolateral overlap is expanded dorsally and may be continuous with an overlap for the posterior dorsolateral plate). The dorsal apex is involved in a

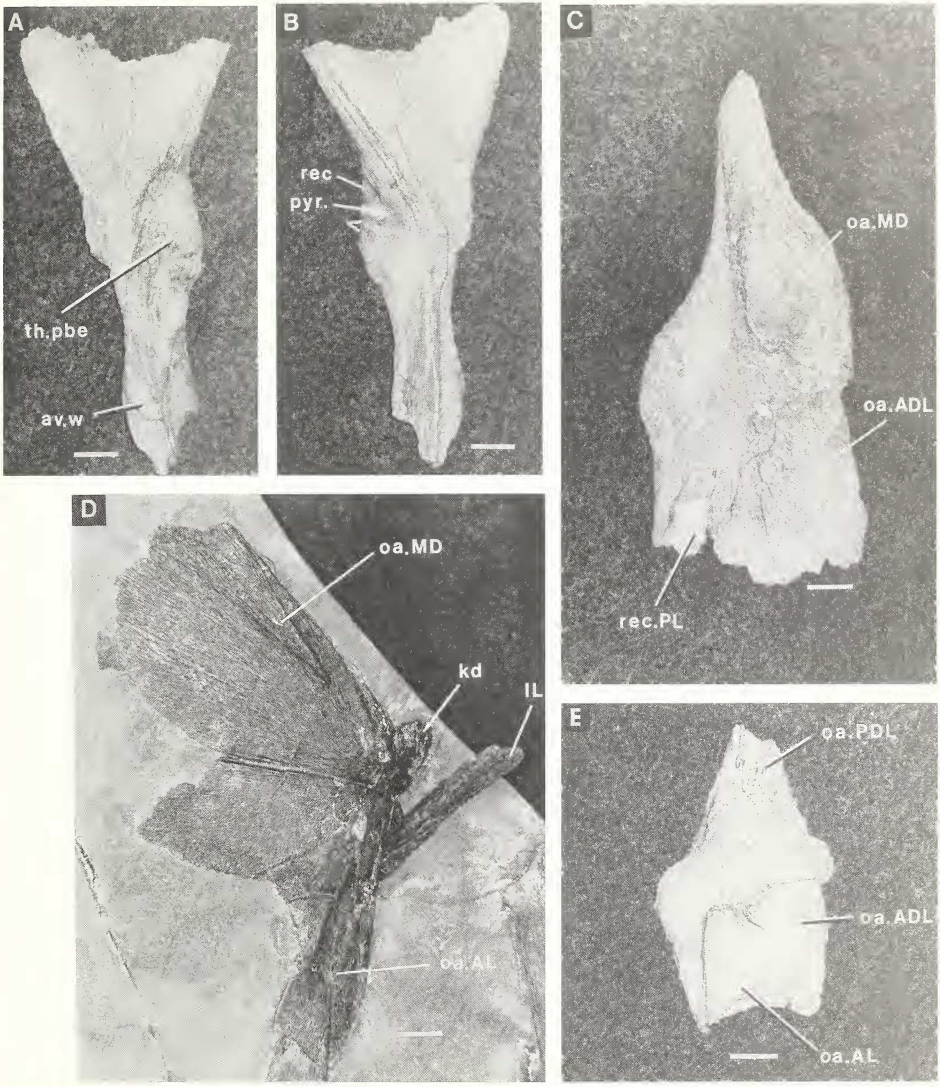

Figure 11. *Gymnotrachelus hydei* (CMNH 8051). Right anterior lateral plate in A, external and B, internal views. Note that the short process forming the anteroventral border of the recess is reconstructed in white. C, right posterior dorsolateral plate in external view. D, right anterior dorsolateral plate in external view and interolateral plate. E, right posterior lateral plate in external view. Scale bars equal 1 cm.

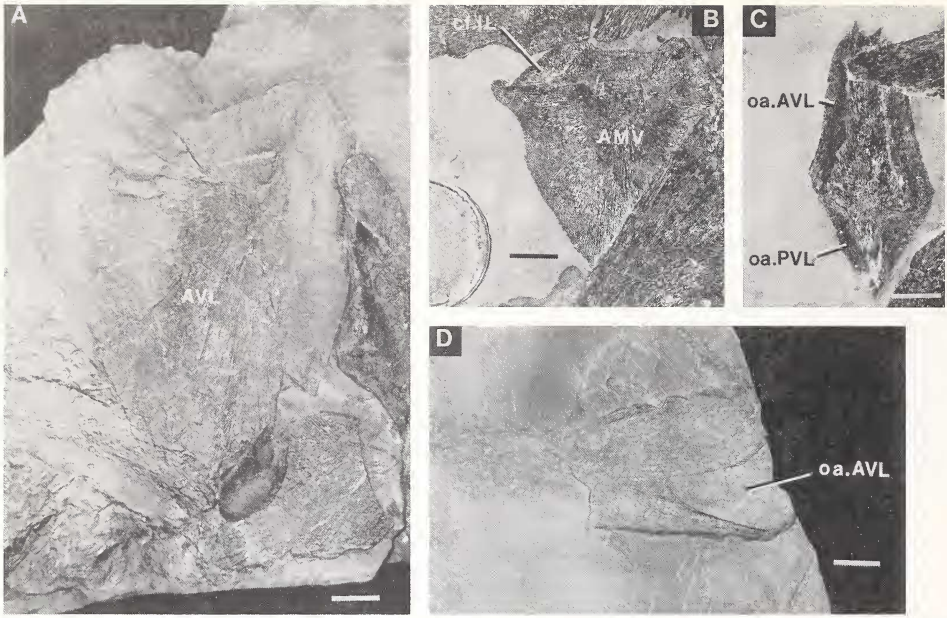

Figure 12. *Gymnotrachelus hydei.* A, right anterior ventrolateral plate in internal view (CMNH 8054). B, anterior median ventral plate in internal view (CMNH 8050). C, posterior median ventral plate in external view (CMNH 8050). D, anterior fragment of left posterior ventrolateral plate in external view (CMNH 8054). Scale bars equal 1 cm.

junction with the posterior dorsolateral plate (oa.PDL, Figure 11E). The exact nature of this junction is unclear, but as noted above may have involved an insertion of the posterolateral plate into the posterior dorsolateral plate (a similar style of junction is seen in *Dunkleosteus*).

Interolateral (IL). A single example of an interolateral plate is seen in CMNH 8051 (Figure 11D). Little can be discerned other than the presence of an elongate plate.

Anterior median ventral (AMV). An anterior median ventral plate (Figures 2C, 12B) is present in CMNH 8050 only and is partially covered and exposed in internal view. The plate is triangular in shape with the base of the triangle anterior (width/length = *ca.* 1.0). The anterior margin possesses two anteriorly directed and rounded projections separated medially by a shallow trough. A contact face for the interolateral plate (cf.IL, Figure 12B) is present laterally on the anterior margin. The anterolateral corners of the plate form short processes. From these processes, the plate narrows to its posterior midpoint with gently convex lateral margins. Compression during preservation of the anterior median ventral plate reveals the presence of large overlap areas for the anterior ventrolateral plates on the external surface.

Posterior median ventral (PMV). The posterior median ventral plate (Figures 2C, 12C) is diamond shaped (length/width = *ca.* 2.2). Anterior ventrolateral plate overlap areas (oa.AVL, Figure 12C) extend *ca.* 66% the length of the posterior median ventral plate with overlap areas for the posterior ventrolateral plates (oa.PVL, Figure 12C) extending the remaining portion of the plate. The posterior overlap area is deeper than the anterior one reflecting the overlap pattern of the anterior and posterior ventrolateral plates (the posterior ventrolateral plate overlies the anterior ventrolateral plate).

Anterior ventrolateral (AVL). The anterior ventrolateral plate (Figures 2C, 12A) is longer than wide (length/width = *ca.* 1.3) with the greatest width opposite the ossification center (it is noteworthy that the plate shape and presence of growth ridges strongly resemble the posterior ventrolateral plate in *Heintzichthys gouldii,* Carr, 1991, fig. 14B. There is no question as to the correct interpretation of plates in both forms based on overlap patterns). A thickening is present at the ossification center; however, the Y-shaped thickenings seen in other forms are not discernible (e.g.,

seen in *Eastmanosteus calliaspis,* Dennis-Bryan, 1987, and *Heintzichthys gonldii,* Carr, 1991). Concentric growth ridges are present on the internal surface.

Posterior ventrolateral (PVL). There are no complete posterior ventrolateral plates (Figures 2C, 12D) that clearly show both an anterior and posterior margin (with the possible exception of a right plate with a dislocated posterior fragment on CMNH 8049). CMNH 8799 possesses nearly complete plates with the posterior portion missing. This specimen shows the posterior ventrolateral plates to be greater than three times longer than wide (length/width = *ca.* 3.3). CMNH 8049 is nearly five times longer than wide (length/width = *ca.* 4.9) and appears to represent a younger specimen with fewer growth ridges on the posterior ventrolateral plate. On the basis of CMNH 8049, the posterior ventrolateral plate tapers to a fine posterior point. Ossification centers are located at midplate close to the medial margin.

Internally, growth ridges are present and on CMNH 8049 a contact face for the left posterior ventrolateral plate is present on the medial margin of the right plate (this overlap pattern is opposite to that seen in *Dunkleosteus* and *Heintzichthys,* Carr, 1991, fig. 12B). Externally there is an anterior ventrolateral plate overlap area which is exposed in CMNH 8054 only (oa.AVL, Figure 12D). Similar elongate posterior ventrolateral plates are seen in an undescribed selenosteid from the Cleveland Shale.

Pectoral and Pelvic Fins, Axial Skeleton, and Neurocranium

General features. The pelvic fins, axial skeleton, and neurocranium are not preserved. A perichondrally ossified scapulocoracoid is present. Additional unidentifiable perichondral fragments are present.

Scapulocoracoid. Recognizable scapulocoracoids are present in CMNH 8047 and CMNH 8799. Although incomplete and highly fragmented, the scapulocoracoid appears to be relatively large and nearly equidimensional (length/height = *ca.* 1.1). Numerous neurovascular foramina are present on both the internal and external surfaces. An articular ridge and basals are not discernible on the available material.

Phylogenetic Discussion

The relationships of the North American genera of selenosteid arthrodires remain unresolved. Dunkle and Bungart (1939) noted affinities between *Gymnotrachelus* and *Stenosteus, Selenosteus, Trachosteus,* and *Mylostoma,* although they deferred any definitive assignment. Lelièvre et al. (1987) suggested a sister group relationship between *Gymnotrachelus* and European selenosteids, in part, but did not consider the remaining North American selenosteids. Carr (1991) suggested that *Gymnotrachelus* is a member of an unresolved multichotomy with other aspinothoracid arthrodires and proposed that *Selenosteus* is related more closely to European forms (*Gorgonichthys, Heintzichthys, Gymnotrachelus* (*Selenosteus* (*Pachyosteus, Rhinosteus*))). Denison (1978) noted the uniqueness of European and North American forms, but it is not clear whether he is suggesting that North American forms are monophyletic or is suggesting a relationship equivalent to those proposed by Lelièvre et al. (1987) or Carr (1991). Each of the above hypotheses is consistent with the hypothesis that North American and European selenosteids represent distinct monophyletic groups, but none provide conclusive evidence. Lelièvre et al. (1987) failed to analyze additional North American taxa. Carr (1991), while adding an additional North American taxon, failed to include most of the European forms. Denison (1978), in suggesting the monophyly of these two groups, failed to provide any diagnosis or phylogenetic analysis. While a final revision of selenosteid arthrodires must await the additional description of unpublished North American materials and a review of European selenosteids, new material for *Gymnotrachelus* allows a more definitive analysis of its position within the clade.

An analysis of nine aspinothoracid arthrodiran taxa (after Lelièvre et al., 1987: *Gymnotrachelus, Melanosteus, Rhinosteus, Pachyosteus, Enseosteus, Microsteus, Brannosteus,* Brachydeiridae, and Trematosteidae) using 15 characters gives two equally parsimonious trees (exhaustive search option, treelength = 19, consistency index = 0.737). Trematosteidae and Brachydeiridae are designated as outgroup members.

Characters 1-14 are taken from Lelièvre et al. (1987) with one additional character added to the analysis and are as follows:

1. Submarginal plate shape and orientation (Lelièvre et al., 1987): elongate (0); raised and reduced (1).
2. Postnasal plate fused to preorbital plate (Lelièvre et al., 1987): absent (0); present (1).
3. Marginal plate forms part of orbit margin (Lelièvre et al., 1987): absent (0); present (1).
4. Position of the preorbital-postorbital-central plate junction (Lelièvre et al., 1987): at a level over the anterior half of the orbit (0); posterior half of orbit (1).
5. Angle formed by the postorbital and otic branches of the infraorbital sensory line grooves (Lelièvre et al., 1987): open (0); closed (1).
6. Length of cheek and head shield contact, independent of overlapping or fusion of these two dermal units (Lelièvre et al., 1987): long (0); short (1).
7. Nature of inferognathal and posterior superognathal occlusal surfaces (Lelièvre et al., 1987): trenchant or rounded (0); denticulate (1).
8. Posterior ventrolateral and posterior median plates (Lelièvre et al., 1987): present (0); absent (1).

9. Position of the dermal articulation between the head and thoracic shields (modified from Lelièvre et al., 1987): dorsolateral (0); displaced ventrally (1).
10. Dorsal process on the posterior superognathal plate (Lelièvre et al., 1987): present (0); absent (1).
11. Form of the anterior lateral plate (Lelièvre et al., 1987): infraobstantic region of plate short (0); infraobstantic and postbranchial region elongate with the dorsal region narrow (1).
12. Lingiform process on the suborbital plate (modified from Lelièvre et al., 1987): present (0); reduced (1). This character has been scored as in Lelièvre et al. (1987), although absence of a lingiform process is reinterpreted here as a reduction. The presence of a lingiform process may represent a plesiomorphic feature for the aspinothoracid arthrodires. Recognition of this process in lateral view may reflect the size of the subautopalatine crista (cr.sau, Figure 6B; Carr, 1991) and whether, when secondarily flattened during preservation, the process extends below the ventral external border of the suborbital plate. This crista is often thin and easily lost unless reinforced to form a contact face with the posterior superognathal as seen in *Dunkleosteus* and *Eastmanosteus calliaspis* (cf.PSG, Carr, 1991, fig. 7B).
13. Overlap between the head and cheek dermal plates (Lelièvre et al., 1987): absent (0); present (1).
14. Prehypophysial region of parasphenoid plate elongate and stem-like (modified from Lelièvre et al., 1987): absent (0); present (1).
15. Supraethmoid thickening (th.seth, Stensiö, 1963, figs. 113A, B): absent (0); present (1).

A data matrix for the nine taxa and 15 characters used in the current analysis is provided below. ? = missing data; – = case where the character is not applicable.

Trematosteidae	1 1 0 1 0	0 0 0 0 0	0 0 0 0 0
Brachydeiridae	1 0 1 1 0	0 0 1 0 0	0 0 1 0 ?
Gymnotrachelus	1 – 0 0 1	1 1 0 0 1	1 1 0 1 0
Enseosteus	1 0 1 0 1	1 1 0 1 0	0 0 ? 0 1
Microsteus	1 0 1 0 1	1 1 0 1 0	0 1 1 0 1
Pachyosteus	1 0 1 0 1	1 1 0 0 1	0 0 1 0 ?
Rhinosteus	1 0 1 0 1	1 1 0 0 1	1 1 1 0 ?
Melanosteus	? 0 ? 0 1	1 1 0 0 1	1 1 ? 1 1
Braunosteus	? 1 1 0 0	0 0 0 0 0	0 0 1 0 ?

Family Selenosteidae

(Selenosteidae Dean, 1901; Pachyosteidae Gross, 1932; Braunosteidae Stensiö, 1959, and Rhinosteidae Stensiö, 1963; Selenosteidae Denison 1978; Selenosteidae Lelièvre et al., 1987)

Selenosteidae is a subgroup of the monophyletic aspinothoracid arthrodires (Miles and Dennis, 1979; Gardiner and Miles, 1990; Carr, 1991; but contrast Denison, 1984) that shares with other members of this larger clade a reduction of the lateral and occipital thickenings of the head shield and loss of the spinal plate (Carr, 1991). Denison (1978) united *Braunosteus, Enseosteus, Microsteus, Pachyosteus, Rhinosteus, Gymnotrachelus, Paramylostoma, Selenosteus,* and *Stenosteus* in the family Selenosteidae based on the presence of large orbits, long central plates (relative to preorbitals), short submarginal plates, and a large nuchal gap between the head and thoracic shields. Lelièvre et al. (1987) analyzed better known members of this clade (*Gymnotrachelus, Melanosteus, Rhinosteus, Pachyosteus, Enseosteus, Microsteus,* and *Braunosteus*) along with the outgroups Trematosteidae and Brachydeiridae and excluded *Braunosteus* from the Selenosteidae.

Although a full comparison of analyses by Lelièvre et al. (1987) and Carr (1991) is not practical at present since many of the additional characters used by Carr cannot be evaluated readily using published accounts, some patterns do emerge. The character analyses for *Gymnotrachelus* by Lelièvre et al. (1987) were limited by the material available at the time (the holotype described by Dunkle and Bungart, 1939). Dunkle and Bungart's (1939) reconstruction and plate identifications were flawed, in part, due to poor preservation. Seven of 14 characters interpreted by Lelièvre et al. (1987, characters 1, 6, 7, 10-12, 14) as being primitive are seen to be derived, on the basis of more complete material. Consequently, the analysis of phylogenetic relationships is altered. *Gymnotrachelus* is now recognized as a derived member of the selenosteid clade. A phylogenetic analysis of the taxa reviewed by Lelièvre et al. (1987; Trematosteidae and Brachydeiridae here set as outgroups) suggests the following relationships: (Trematosteidae, Brachydeiridae, *Braunosteus*) ((*Microsteus, Enseosteus*) (*Pachyosteus,* (*Rhinosteus* (*Melanosteus, Gymnotrachelus*)))).

Lelièvre et al. (1987) and the current study concur that the group Selenosteidae *sensu* Lelièvre et al. (1987; Figure 13) is characterized by the presence of: (1) enlarged orbits associated with a closed angle between the postorbital and otic branches of the infraorbital sensory line and a reduction of the contact between the cheek and head shield (characters 5 and 6, Lelièvre et al., 1987) and (2) inferognathals and posterior superognathals possessing denticles along their occlusal surfaces in adults (character 7, Lelièvre et al., 1987).

Within the family, *Melanosteus* and *Gymnotrachelus* are united by the presence of a parasphenoid with a narrow stem-like prehypophysial region (Figure 13; character 14, modified from Lelièvre et al., 1987).

Synapomorphies uniting *Rhinosteus* with the previous clade (*Melanosteus* and *Gymnotrachelus*) are the form of the anterior lateral plate (elongate and dorsally narrow, Figure 13; character 11, Lelièvre et al., 1987) and reduction of the linguiform process on the suborbital plate (Figure 13; character 12, modified from Lelièvre et al., 1987, who in contrast consider the loss of a linguiform process). The definition for a linguiform process needs refinement to distinguish between a subautopalatine crista (cr.sau, Figure 6B; see also Carr, 1991) and a linguiform process that appears to include a ventrally visible subautopalatine crista, which may or may not possess reinforcement for a posterior superognathal contact face (cf.PSG, Carr, 1991, fig. 7B).

Uniting *Pachyosteus* with the above clade is the loss of a dorsal process on the posterior superognathal (Figure 13; character 10, Lelièvre et al., 1987).

Microsteus and *Enseosteus* share a ventral position for the dermal articulation between the head and thoracic shields (Figure 13; character 9, Lelièvre et al., 1987; see also Miles, 1969). Additionally, they possess a supraethmoid thickening (character 15; th.seth, Stensiö, 1963, fig. 113A & B; independently derived in *Melanosteus*, Lelièvre et al., 1987, fig. 3). The presence of this feature is primitive, with Trematosteidae and *Gymnotrachelus* independently losing the supraethmoid thickening. However, members of immediate outgroups (e.g., *Dunkleosteus* and *Heintzichthys*) lack a supraethmoid thickening. Based on a parsimony argument, the presence of a supraethmoid thickening is a derived feature known only in *Enseosteus, Microsteus,* and *Melanosteus.* This region of the head shield is not known in Brachydeiridae, *Rhinosteus, Pachyosteus,* and *Braunosteus.*

One of the two equally parsimonious trees derived from the current study contains a monophyletic Selenosteidae *sensu* Denison (1978), which includes *Braunosteus.* The alternative hypothesis agrees with Lelièvre et al. (1987) placing Brachydeiridae as the sister group to selenosteids, but leaves unresolved the relationship of *Braunosteus.* Selenosteidae *sensu* Denison (1978) is characterized by an anterior shift of the triple point formed by the junction of central, preorbital, and postorbital plates (character 4, Lelièvre et al., 1987). In the alternative tree, a Brachydeiridae-Selenosteidae clade is characterized by the loss of fusion between the postnasal plate and head shield. The latter hypothesis suggests that fusion of the postnasal is a primitive feature. As noted above for the supraethmoid thickening, a consideration of additional outgroups suggests that the fusion of the postnasal plate represents a derived feature which is either independently evolved in Trematosteidae and *Braunosteus* or represents a synapomorphy for the two taxa. The absence of fusion in basal eubrachythoracid arthrodires gives a weak criterion for choosing between

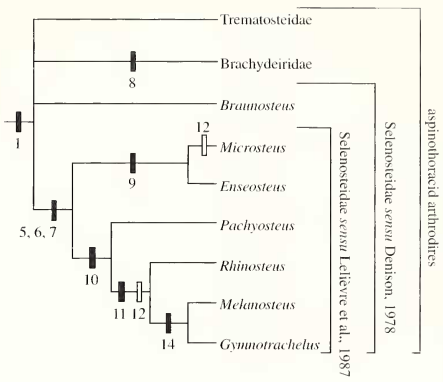

Figure 13. A strict consensus tree based on two trees derived from PAUP (two trees found with exhaustive search, treelength = 19, consistency index = 0.737). Trematosteidae and Brachydeiridae are designated as outgroup members. Unambiguous character transformations are indicated as follows: unique, black filled rectangles and homoplasic, open rectangles. Characters 1 and 8 are uninformative.

these two equally parsimonious trees. Selenosteidae *sensu* Denison may represent a more appropriate depiction of the relationship of *Braunosteus* (i.e., a basal selenosteid arthrodire). The phylogenetic position of *Braunosteus* is sensitive to the choice of additional outgroups. A final resolution of the relationship of *Braunosteus* is beyond the scope of this paper.

Denison (1978) considered three additional North American taxa as members of the Selenosteidae that are not considered in the current study (*Selenosteus, Stenosteus,* and *Paramylostoma*). *Selenosteus* and *Stenosteus* share with *Gymnotrachelus* a uniquely shaped median dorsal plate with pronounced anterolateral alae. This feature might suggest a close relationship among these taxa. *Paramylostoma,* the remaining selenosteid which is represented by only a few specimens, is too poorly known to analyze adequately. The loss of a posterior process on the posterior superognathal suggests that *Paramylostoma* may be a member of the *Pachyosteus-Rhinosteus-Melanosteus-Gymnotrachelus* group (Figure 13), although this assignment is tenuous at best.

Conclusion

New material for *Gymnotrachelus* affords better resolution of its phylogenetic position within Selenosteidae.

Gymnotrachelus is a derived member of Selenosteidae and is the sister group to *Melanosteus*. The present study has not resolved adequately the relationships of *Braunosteus*, although among alternative hypotheses a parsimony argument suggests that *Braunosteus* is a basal member of Selenosteidae. Analysis of other putative members of Selenosteidae (*Selenosteus, Stenosteus, Paramylostoma*) is only tentative and further analysis must await a review of poorly known taxa and description of new materials. *Selenosteus* and *Stenosteus* are speculatively related to *Gymnotrachelus* while *Paramylostoma* appears to be a member of the *Pachyosteus-Rhinosteus-Melanosteus-Gymnotrachelus* clade.

Acknowledgments

I would like to thank Dr. Michael Williams, The Cleveland Museum of Natural History (CMNH), for access to the bulk of materials used in this study and Gary Jackson (CMNH) for patiently listening to arguments for the interpretations of problematic materials. Additionally, I want to thank Dr. John Ostrom for the loan of material from the Peabody Museum, Yale University; and Rob Cox and Drs. Carl Gans, Daniel Goujet, Hervé Lelièvre, Hans-Peter Schultze, and Gerald R. Smith for their reviews of the manuscript. This report was submitted in partial fulfillment of the requirements for a Doctor of Philosophy in Geological Sciences in the Horace H. Rackham School of Graduate Studies at The University of Michigan.

References

Carr, R. K. 1991. Reanalysis of *Heintzichthys gouldii*, an aspinothoracid arthrodire (Placodermi) from the Famennian of northern Ohio, U.S.A. with a review of brachythoracid systematics. Zoological Journal of the Linnean Society, 103:349-390.

Denison, R. H. 1975. Evolution and classification of Placoderm fishes. Breviora, 432:1-24.

Denison, R. H. 1978. Handbook of Paleoichthyology. 2. Placodermi. Stuttgart: Gustav Fischer Verlag.

Denison, R. H. 1984. Further consideration of the phylogeny and classification of the Order Arthrodira (Pisces: Placodermi). Journal of Vertebrate Paleontology, 4:396-412.

Dennis-Bryan, K. D. 1987. A new species of eastmanosteid arthrodire (Pisces: Placodermi) from Gogo, Western Australia. Zoological Journal of the Linnean Society, 90:1-64.

Dennis, K. D., and R. S. Miles. 1979. Eubrachythoracid arthrodires with tubular rostral plates from Gogo, Western Australia. Zoological Journal of the Linnean Society, 67:297-328.

Dunkle, D. H., and P. A. Bungart. 1939. A new arthrodire from the Cleveland Shale Formation. Scientific Publications of The Cleveland Museum of Natural History, 8:13-28.

Gardiner, B. G. 1990. Placoderm fishes: diversity through time, p. 305-319. In P. D. Taylor and G. P. Larwood (eds), Major Evolutionary Radiations. Oxford: Clarendon Press.

Gardiner, B. G., and R. S. Miles. 1990. A new genus of eubrachythoracid arthrodire from Gogo, Western Australia. Zoological Journal of the Linnean Society, 99:159-204.

Goujet, D. 1984. Les Poissons Placodermes du Spitzberg. Arthrodires Dolichothoraci de la Formation de Wood Bay (Dévonien Inférior). Paris: Cahiers de Paléontologie.

Gross, W. 1932. Die Arthrodira Wildungens. Geologische und Palaeontologische Abhandlungen 19:1-60.

Heintz, A. 1932. The structure of *Dinichthys*, a contribution to our knowledge of the Arthrodira. Bashford Dean Memorial Volume, Archaic Fishes, 4:115-224.

Lelièvre, H., R. Feist, D. Goujet, and A. Blieck. 1987. Les vertébrés dévoniens de la Montagne Noire (sud de la France) et leur apport à la phylogénie des pachyostéomorphes (Placodermes Arthrodires). Palaeovertebrata 17:1-26.

Maddison, W. P., and D. R. Maddison. 1992. MacClade: Analysis of phylogeny and character evolution. Version 3. Sinauer Associates, Sunderland, Massachusetts.

Miles, R. S. 1969. Features of placoderm diversification and the evolution of the Arthrodire feeding mechanism. Transactions of the Royal Society of Edinburgh, 68:123-170.

Miles, R. S., and K. D. Dennis. 1979. A primitive eubrachythoracid arthrodire from Gogo, Western Australia. Zoological Journal of the Linnean Society, 65:31-62.

Obruchev, D. V. 1964. Class Placodermi. Fundamentals of Paleontology. XI. Moscow (in Russian; translated into English by the Israel Program for Scientific Translations in 1967).

Stensiö, E. A. 1963. Anatomical studies on the arthrodiran head. Part I. Preface, geological and geographical distribution, the organization of the head in the Dolichothoraci, Coccosteomorphi, and Pachyosteomorphi. Taxonomic appendix. Kungliga Svenska Vetenskapsakademiens Handlingar, 9:1-419.

Stensiö, E. A. 1969. Anatomie des arthrodires dans leur cadre systématique. Annales de Paléontologie, 55:151-192.

Swofford, D. L. 1993. PAUP: Phylogenetic Analysis Using Parsimony, Version 3.1. Computer program distributed by the Illinois Natural History Survey, Champaign, Illinois.

Abbreviations Used in Text and Figures

a.Au	depression for autopalatine
ADL	anterior dorsolateral plate
AL	anterior lateral plate
AMV	anterior median ventral plate
ant.	anterior
ASG	anterior superognathal
AVL	anterior ventrolateral plate
av.w	anteroventral wing
C	central plate
cf.IL	contact face for interolateral plate
cf.PSO	contact face for postsuborbital plate
ch.pro.pr	channel for dorsal aspect of preorbital process of neurocranium
ch.pr.sv	channel for dorsal aspect of supravagal process of neurocranium
cr.po	postocular crista

cr.pr	carinal process
cr.sau	subautopalatine crista
cr.so	subocular crista
csc	central sensory line groove
d.end.e	external opening for the endolymphatic duct
f_e.lv	elongate fossa for levator muscle of head
IG	inferognathal
IL	interolateral plate
ioc.ot	otic branch of infraorbital line groove
ioc.pt	postorbital branch of infraorbital line groove
ioc.sb	suborbital branch of infraorbital line groove
kd	glenoid condyle
laf	lateral articular fossa
lc	main lateral line
M	marginal plate
MD	median dorsal plate
med.	medial
m.sept	median septum
n.th	nuchal thickening
Nu	nuchal plate
oa.ADL	overlap area for anterior dorsolateral plate
oa.AL	overlap area for anterior lateral plate
oa.AVL	overlap area for anterior ventrolateral plate
oa.C	overlap area for central plate
oa.M	overlap area for marginal plate
oa.MD	overlap area for median dorsal plate
oa.Nu	overlap area for nuchal plate
oa.PL	overlap area for posterior lateral plate
oa.PNu	overlap area for paranuchal plate
oa.PrO	overlap area for preorbital plate
oa.PtO	overlap area for postorbital plate
oa.PVL	overlap area for posterior ventrolateral plate
oa.SM	overlap area for submarginal plate
oa.SO	overlap area for suborbital plate
P	pineal plate
pap	occipital para-articular process
PDL	posterior dorsolateral plate
PL	posterior lateral plate
PM	postmarginal plate
PMV	posterior median ventral plate
PNu	paranuchal plate
pp	posterior pit-line groove
p.pr	median posterior process
pre.reg	prehypophysial region
PrO	preorbital plate
PSG	posterior superognathal
PSO	postsuborbital plate
PtO	postorbital plate
pt.u	paired pits on visceral surface of nuchal plate
PVL	posterior ventrolateral plate
pyr.	pyrite nodule
Qu	position of quadrate
R	rostral plate
rec	recess
rec.PL	collapsed recess for the posterior lateral plate
scler	sclerotic plate
SM	submarginal plate
SO	suborbital plate
soc	supraorbital sensory line groove
sorc	supraoral sensory line groove
suo.v	supraorbital vault
th.pbe	thickening within the postbranchial embayment
?	unknown plate fragment
1	postscript denoting a left element
2	postscript denoting a right element